

湖南大学学报（自然科学版）
Journal of Hunan University (Natural Sciences)

第 49 卷 第 12 期
2022 年 12 月

Available online at http://jonuns.com/index.php/journal/index

Vol. 49 No. 12
December 2022

Open Access Article

https://doi.org/10.55463/issn.1674-2974.49.12.14

Crystal Structure and Magnetic Properties of Fe_3O_4 Nanoparticles Using Iron Sand as a Raw Material for Mercury Removal

Nurhasana Siregar[1], Kurnia[2*], Budhy Kurniawan[3], Margaretha Tabita Tuny[4], Joko Utomo[5], Bayu Achil Sadjab[2], Delpia Susu[2], Susan Adrianti Gambe[2]

[1] Department of Civil Engineering, Faculty of Engineering, Universitas Graha Nusantara, Padang Sidimpuan 22733, Indonesia

[2] Department of Physics, Faculty of Mathematics and Natural Sciences, Universitas Halmahera, Tobelo, Maluku Utara 97762, Indonesia

[3] Department of Physics, Faculty of Mathematics and Natural Sciences, Universitas Indonesia, Jakarta 16424, Indonesia

[4] Department of Forestry, Faculty of Mathematics and Natural Sciences, Universitas Halmahera, Tobelo, Maluku Utara 97762, Indonesia

[5] Department of Physics, Faculty of Mathematics and Natural Sciences, Universitas Negeri Malang, Jawa Timur 65145, Indonesia

* Corresponding author: kurniakurniarahman@gmail.com

Received: August 16, 2022 / Revised: October 11, 2022 / Accepted: November 13, 2022 / Published: December 30, 2022

Abstract: Fe_3O_4 nanoparticles based iron sand from Maluku Utara have been successfully synthesized by co-precipitation methods with varying of the synthesis temperature by 50°C, 60°C and 70°C. The crystal structures and magnetic properties were characterized using X-ray Diffraction (XRD) and Vibrating Sample Magnetometer (VSM). The XRD showed that the Fe_3O_4 samples have a single phase invers spinel cubic structure. The Crystalization of the temperature 70°C is better than 50°C and 60°C, with the intensity peak index of 311 of 42.688 a.u, whereas at the temperature of 60°C and 50 °C are 25.731 a.u and 22.719 a.u, respectively. There's no increase in crystallite size with increasing synthesis temperature, with each sizes 23.047 nm, 24.043 nm and 16.041 nm respectively. The VSM showed that the Fe_3O_4 samples are soft-ferrimagnetic. The M_r and M_{max} are higher at 70°C than 60 °C and 50°C by 3,785 emu/gr 20,288 emu/gr (70°C), 2,432 emu/gr 14,713 emu/gr (60°C), 1.473 emu/gr 12.519 emu/gr (50°C). The coercivity *Hc* at 70°C and 60°C relatively identical at 0.011 T, whereas at 50°C *Hc* is 0.012 T. The nanoparticles that are synthesized at 70°C are selected for mercury removal due to their stable crystallinity and good magnetic properties. The nanoparticles were able to remove mercury with an adsorption capacity 0,45 mg/g and easy to separate it from the solution.

Keywords: magnetic properties, crystal structure, iron sand, mercury removal.

以铁砂为原料除汞的四氧化三铁纳米粒子的晶体结构和磁性能

摘要：采用共沉淀法成功合成了来自马鲁古北的四氧化三铁纳米颗粒铁砂，合成温度分别为 50 摄氏度、60 摄氏度和 70 摄氏度。使用 X 射线衍射和振动样品磁强计表来征晶体结构和磁性。X 射线衍射表明四氧化三铁样品具有单相反的尖晶石立方结构。70 摄氏度结晶优

© 2022 by the authors. This article is an open access article distributed under the terms and conditions of the Creative Commons Attribution (CC-BY) license (http://creativecommons.org/licenses/by/4.0/).

于 50 摄氏度和 60 摄氏度，强度峰值指数为 311，为 42.688 原子单位，而 60 摄氏度和 50 摄氏度分别为 25.731 原子单位和 22.719 原子单位 ，分别。随着温度的升高，微晶尺寸没有增加，每个尺寸分别为 23.047 纳米、24.043 纳米和 16.041 纳米。振动样品磁强计表明四氧化三铁样品是软亚铁磁性的。剩余磁化强度和最大磁化强度在 70 摄氏度时比 60 摄氏度和 50 摄氏度高 3,785 电磁单位/克 20,288 电磁单位/克（70 原子单位），2,432 电磁单位/克 14,713 原子单位/克（60 摄氏度），1.473 电磁单位/克 12.519 电磁单位/克（50 摄氏度）。70°C 和 60°C 的矫顽力相对一致，为 0.011T，而 50°C 的矫顽力为 0.012T。70°C 合成的纳米粒子结晶稳定，磁性能好，被选作除汞用。纳米颗粒能够以 0.45 毫克/克的吸附能力去除汞，并且易于将其与溶液分离.

关键词：磁性, 晶体结构, 铁砂, 除汞.

1. Introduction

Mercury pollution at high concentrations can represents an important threat to human health and ecological systems [1–2]. Mercury (II) has high toxicity, persistent character in the environment and biomagnifications through the food chain [3]. The maximum allowable level for mercury (II) in surface water is 0,07 μg/L [4]. Mercury (II) is delivered into the environmental by textile industries, ilegal mining and smelting, burning of fossils fuels and chlor-alkali plants [5–7]. Accordingly, extensive studies have been performed to discover the mercury (II) removal process that incorporates precipitation, membrane filtration, ion exchange and adsorption [8–11]. Among the remediaton process, adsorption with the fitted adsorbents have prosses fast rate, large capacity, and high selectivity for harmful metal ions. Recently adsorbent for water treatment have used magnetic materials such as Fe3O4 [12–15].

Nanoparticles have attracted the attention of researchers because of their potential for industrial, biomedical, and environmental applications, such as improving polluted water, soil and air [16]. Fe_3O_4 nanoparticles have unique properties, such as surface area, high surface energy, low toxicity, good biocompatibility, superparamagnetic, ferromagnetic, ferromagnetic magnetic properties, high absorption rate, and electron-electron transfer. [17–22].

The properties of nanoparticles can be influenced by the synthesis method, and synthesis parameters such as synthesis time, synthesis temperature, NaOH catalyst, and post-synthetic actions such as anneling and calcination [23–24]. Fe_3O_4 nanoparticles based on natural iron sand have been synthesized by precipitation, coprecipitation, coprecipitation-ultrasonic irradiation methods, High Energy milling (HEM), ball milling [20, 25-27]. The coprecipitation method can produce smaller crystallite sizes compared to other synthesis methods, and in terms of cost, it is relatively cheap. Iron sand is a mineral that is widely found in Indonesia, especially in Wari, Maluku Utara. The total volume of iron sand deposited in Wari beach reaching 405.335 m^3 that measured using geo electricity to explore the distribution and volume of the iron sand both for mapping and sounding methods. Iron sand in Wari contains 73,4 % Fe, Si, Ca, Ti, Al, K and other elements based on the X-Ray Fluoresence Data [28]. Iron sand is a raw material that can be synthesized to be Fe_3O_4 nanoparticles that has a spinel ferrite structure [29]. The results of this exploration are expected to be used either for advanced material technology or for increasing the value of the iron sand commodity in Wari. Iron sand can be used as the basic material for the manufacture of nanoparticles. Additionally, iron sand can be dominated by iron oxides such as magnetite Fe_3O_4, maghemite α– Fe_3O_4, hematite γ–Fe_3O_4, and magnetite Fe_3O_4 which are the strongest magnetic material [25]. Fe_3O_4 nanoparticle properties for mercury removal are influenced by microstructure, morphology and crystallite size [30]. Microstructure includes crystal structure, crystal phase, lattice parameters and crystal density. The crystallite size and crystallinity of a nanoparticle can be controlled by the synthesis temperature. The crystallite size can influence the magnetic properties of nanoparticles [31]. The magnetic properties of Fe_3O_4 come from Fe^{2+} and Fe^{3+}. Iron sand is one source of magnetite, namely, ferrous ferrite ($Fe[Fe_2O_4]$), which occurs naturally [32]. Magnetite has been used as a magnetic nanocomposite material to absorb waste in wastewater [25]. Therefore, this study synthesized nanoparticles based on Wari beach sand, North Halmahera using the coprecipitation method with variations in synthesis temperature order to analyze the crystal structure and magnetic properties of Fe_3O_4 nanoparticles. The Fe_3O_4 magnetic nanoparticles products are expected to be used as a basic material that will be applied to remove mercury waste in water.

2. Experiment

2.1. Materials

Iron sand from Wari Beach, HCl 37% Merck Emsure, NaOH, Merck Hg(NO3)2 Merck Emsure. All chemicals were used without purification.

2.2. Collection of Iron Sand

Iron sand was taken from Wari beach purposively. The sand was washed again using water and dried. repeated 3 times, then 50 g of sand was washed again using distilled water and dried at 100^0C for 1 hour.

2.3. Synthesis of Fe3O4 Nanoparticles

Fe3O4 nanoparticles were synthesized by co-precipitation method using iron sand as a raw material from Wari Beach in Halmahera Utara, Maluku Utara. First the the iron sand was extracted with HCl in a ratio of 1:2 and sintered at a temperature of 55°C for 10 min. Then, the results of the iron sand solution with HCl were filtered and dripped slowly into NaOH (3 M) at the synthesis temperature 50 °C, 60 °C and 70°C, for an hour. Then, a blackish brown solid liquid is formed, after the sample was in slurry form. Later the sample was puy into an oven with a calcination temperature of 100°C for 3 hours. The obtained samples were characterized using XRD to determine the crystal structure and size of the crystallites, and to determine the magnetic properties of the material-used VSM with room temperature settings and an external field of 1 Tesla.

2.4. Mercury Adsorption

0.1 g of Fe_3O_4 nanoparticles is placed in an Erlenmeyer flask that contains 30 ppm. Using mercury solution standard MERCK 1000 ppm that diluted to 30 ppm. The solution was shaken at 150 rpm for 80 min. After adsorption, the Fe_3O_4 nanoparticles were separated using a permanetnt magnet. After AAS analyses adsorption nanoparticle, the adsorption capacity is determined using Equation 1

$$Q = \frac{(Ci - Ce)V}{W} \quad (1)$$

where Ci is the intial concentration of Hg, Ce is the concentration in equilibrium. W is weight of adsorbent and V is the volume of Hg solution.

2.5. Characterization

The X-Ray diffraction pattern of Fe_3O_4 nanoparticles was determined on an X-Ray Diffractometer PANalytical Type X'Pert Pro using 2θ = $(10–90)^0$. The magnetic properties of the nanoparticles were determined on a Vibrating Sample Magnetometer Oxford type 1,2H, SEM EDX FEI Type Inspect-S50, AAS Cold Vapor Varian AA240FS.

3. Result and Discussion

3.1. X-Ray Diffraction Analysis

The sample obtained at synthesis temperature 70°C formed blackish brown colored Fe_3O_4 nanoparticles, while at 60°C and 50°C formed brown Fe_3O_4 nanoparticles. The sample at 70°C has a better response to magnets than samples at 50°C and 60°C. XRD results of Fe_3O_4 nanoparticles are shown in Figure 1. The XRD pattern shows invers cubic spinel structure with JCPDS No. 19–0629. and the higher the synthesis temperature, the higher the degree of crystallinity, Fe_3O_4 nanoparticles at synthesis temperature 70°C (42.688 au) the crystallinity is higher than at 60°C (25.731 au) and 50°C (2"2.719 au). The phase formed of Fe_3O_4 nanoparticles from wari beach was a single Fe_3O_4 phase, in this result agrees with the report by [28, 33]. The diffraction peaks (220), (311), (400), (511), (440) showed relatively no 2 theta shift at either temperature 50°C, 60°C and 70°C.

Fe_3O_4 nanoparticles have a cubic crystal structure, the molecular formula Fe_3O_4 is written as $(Fe^{2+})(Fe^{3+})_2O_4$ where the Fe^{2+} cations occupy the octahedral sites and the Fe^{3+} cations occupy the tetrahedral and octahedral sites, so that a single phase is formed Fe_3O_4 [21].

The diffraction peak at (311) increases with increasing synthesis temperature, and the 2θ position of (311) is shown in Table 1, at 50°C, 60°C and 70°C are about 35.556, 35.531, and 35.510. By the diffraction peak of (311), lattice parameters *a*, density ρ and micro strain ε can be determined using formulae (2), (3) and (4) respectively, which the value are shown in the table 1 and 2. The size of the crystallites is determined using the Scherer equation, and to determine the distance between the planes using the Bragg equation $d \sin\theta = n\lambda$. The XRD diffractometer using Cu K$\alpha = 1.54$ Å.

$$\frac{1}{d^2} = \frac{h^2 + k^2 + l^2}{a^2} \quad (2)$$

$$\rho = \frac{nM}{Na^3} \quad (3)$$

$$\varepsilon = \frac{B}{\tan\theta}. \quad (4)$$

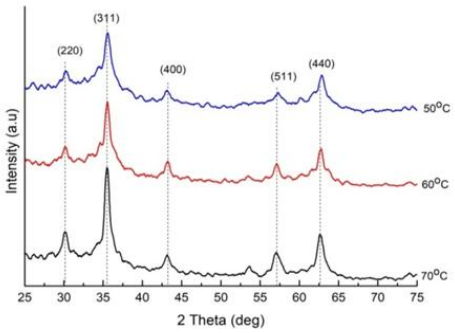


Fig. 1 XRD pattern of Fe_3O_4 nanoparticles for various synthesis temperatures (Developed by the authors, 2022)

Table 1 Lattice parameters and density of Fe_3O_4 nanoparticles

Synthesis Temperature (^{0}C)	A (Å)	ρ (gr/cm^3)
70	8.378	4.771
60	8.373	4.779
50	8.367	4.789

Table 2 Crystallite size and microstrain of Fe3O4 nanoparticles

Synthesis Temperature (^{0}C)	t (nm)	$\varepsilon(nm)$
70	23.047	0.020
60	24.043	0.019
50	16.041	0.028

Figure 2 shows that the Fe_3O_4 nanoparticles have the spherical form. The morphological shows the uniform grain (a) of the Fe_3O_4 after encapsulated, the encapsulation requires for EDX analysis to avoid agglomeration and does not change the structure. In the result it appears that the dominant component was Fe and O. It was confirmed that Fe3O4 was successfully synthesized. The lattice parameters obtained are slightly smaller than the magnetite bulk a = 8,394 [34]. Increasing the synthesis temperature increased lattice parameters, and smaller densities. The relation between lattice parameters and density explains that the greater the distance between atoms in a unit cell, the smaller the atomic density. From the XRD Data Shows that The smallest crystallite size was 16.041 nm, slightly different from the Tedy's crystallite size of 15.70 nm [35]. In table 2, it can be seen that the smaller the size of the crystallites, the more the microstrain increases, causing the diffraction peaks in the plane (311) of the sample at 50^{o}C to widen and shift. The microstrain phenomenon in the sample occurs due to crystal imperfections, which means that there is a uniform strain between the crystal lattices. The higher the synthesis temperature during co-precipitation the larger the crystallite size. The higher the synthesis temperature, the more available thermal energy to causes the atoms to diffuse and vibrate, making the crystal growth become faster and the size tend to be bigger. The best crystallinity is chosen to be applied in mercury solution for mercury adsorption process. A high adsorption rate depends on the good crystallinity of the nanoparticles of Fe3O4 [8–11]. Interactions between mercury and magnetite have not been understood in detail. A Recent reports stated that Hg2+ can be adsorbed on the magnetite surface from HgCl2 solution and converted to Hg0, which is volatile by Fe2+ [36]. The formation of volatile Hg0 is difficult to confirmation but if it happens, it's clearly not detected on XRD. Other research on magnetite shows that the lack of a chloride ion, Hg2+ is reduced to Hg0, whereas in the presence of chlor is in agrees with the current result study. The interaction of Fe species with Hg^{2+} and the redox reaction that produces Hg2Cl2, Hg0, and HgO have been discussed in other studies as well Ions reduced to Hg^+ give Hg_2Cl_2 [37]. The limitation of this study is that the adsorbent needs a combination of polimer materials to improve the adsorption capacity. The main object of this study is to develop magnetic materials that are useful to separating mercury solution from the adsorbent.

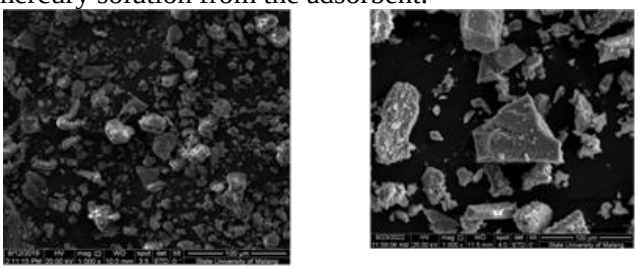


Fig. 2 SEM of the Fe SEM Fe3O4 nanoparticles (a)

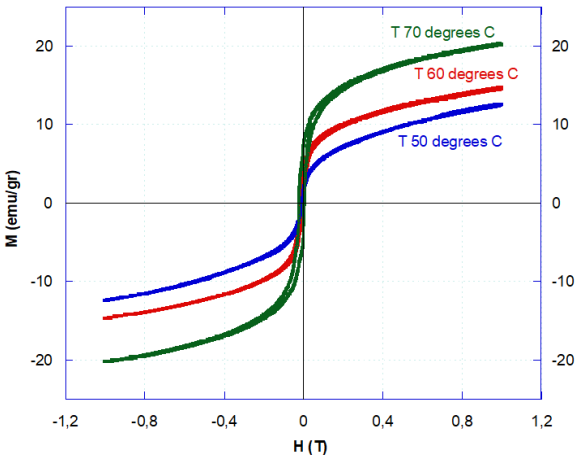


Fig. 3 VSM analysis of Fe3O4 nanoparticles

3.2. VSM Analysis

An external field applied of 1 T results in the hysteresis curve in Figure 3. It appears that samples 50 ^{o}C, 60 ^{o}C, and 70 ^{o}C have not been saturated and can be seen from the shape of the hysteresis, the magnetic loop is narrow. In table 3, the coercivity value is less than 0.03 T, which indicates that the Fe_3O_4 magnet formed is soft magnetic [38]. A magnet that cannot be saturated means that the magnet is not a single domain state. Based on the loop hysteresis in figure 3 (c), Fe_3O_4 nanoparticles synthesized by the coprecipitation method at 70^{o}C synthesis temperature have a higher value of the maximum magnetization (M_{max}), and remanence magnetization (M_r) than at 50 ^{o}C and 60^{o}C synthesis temperature, which are 20.288 emu/gr and 3.785 emu/gr. While the coercivity field (H_c) value at is 0.0110 T, means close to zero, same as the result in [18]. The Fe_3O_4 had superparamagnetic behavior with a Hc value is close to zero [18]. while the relative coercivity is not affected by the synthesis temperature. Judging from the crystallite size, it is not 10 nm, which indicates that the Fe_3O_4 nanoparticles obtained are not superparamagnetic, in contrast to the findings in [20], the size of the nanoparticles obtained this study is larger than 20 nm, and in the form of ferrimagnetic, same as the [22] research. The crystallite size is smaller, the number of domains decreases fewer, so

magnetic moment will decrease and result in a reduction in the maximum magnetization [18]. The relationship between crystallite size and coercivity, the smaller the crystallite size, the higher the coercivity value of sand-based Fe_3O_4 nanoparticles from Wari, Halmahera Utara. The crystallite size of Fe_3O_4 nanoparticles are not single domain relatively because magnetite contains single domain of about 5–20 nm [39]. Based on their magnetic properties, the Fe_3O_4 nanoparticles resulting from this research exhibit promising potential for bioaplication [18,16]. According to the magnetic properties of Fe_3O_4 nanoparticles, they have the potential to separate Fe_3O_4 from the mercury solution after the adsorption process.

3.3. Mercury Removal

Table 4 shows the mercury removal using Fe_3O_4 nanoparticles. The results show that the adsorption capacity of Fe3O4 nanoparticles is relatively low because the magnetite does not have enough electrostatic force during the reaction between Hg2 and Fe3O4. The adsorption process occurred at pH 4. At acidic pH, the formal charge of Fe3O4 changes because the amino group becomes positive, while the mercury ion is also positive, causes a repulsive force to occur adsorption potential reduced due to the formation of compounds with the same charge from the nanoparticles as $(OH)3$ cause repulsion at this surface [40–41] and is dominated by OH-, which reacts with Hg2+ ions to form a precipitated compound, which is not conducive to the adsorption process [42–47].

Table 4 Mercury removal using Fe_3O_4

No.	Co (ppm)	Ce (ppm)	Q (mg/g)
1	30	15	0345

4. Conclusion

Fe_3O_4 nanoparticles have been successfully synthesized based on iron sand using coprecipitation method with various synthesis temperatures, the properties magnetic the M_{max} and H_c values of 20.288 emu/gr and 0.0110T respectively. The higher the synthesis temperature, the higher the degree of crystallinity, but the increase in temperature did not significantly affect the change in crystallite size. The Fe_3O_4 nanoparticles formed have a cubic crystal structure. The results of the VSM characterization show that the smaller the relative crystallite size, the greater the coercivity value of Fe_3O_4 nanoparticles. The nanoparticles produced in this research were soft and ferromagnetic. Nanoparticles that are synthesized at 70^0C are selected to be applied in mercury solution for mercury adsorption process. A high adsorption rate depends on the good crystallinity of the nanoparticles of Fe_3O_4. Good crystallinity is shown by the low of the microstrain value. The magnetic properties of Fe_3O_4 are useful The magnetic properties of the nanoparticles are useful for separating the solution from the adsorbent after the adsorption process using magnet external. Fe_3O_4 nanoparticles have a capacity adsorpsi 0.45 mg/g.

Acknowledgment

The Research was financially supported by Kementerian Pendidikan dan Kebudayaan Riset Pendidikan TinggI on scheme of PKPT in 2021–2022.

References

[1] AZIZI S. N., ROOZBEHANI DEHNAVI A., and JOORABDOOZHA A. Synthesis and characterization of LTA nanozeolite using barely husk silica: Mercury removal from standard and real solutions. *Materials Research Bulletin*, 2013, 48: 1753-1759. https://doi.org/10.1016/j.materresbull.2012.12.068

[2] JIMENEZ-JIMENEZ J, ALGARRA M., RODRIGUEZ-CASTELLON E., JIMENEZ-LOPEZ A. and ESTEVES DA SILVA J. C. G. Hybrid porous phosphate heterostructures as adsorbents of (Hg(II) and Ni (II) from industrial sewage. *Journal of Hazardous Materials*, 2011, 190(1-3): 694-699. https://doi.org/10.1016/j.jhazmat.2011.03.110

[3] ZOLFAGHARI G., ESMAILI-SARI A., ANBIA M., YOUNESI H., AMIRMAHMOODI S., and GHAFARI-NAZARI A. Taguchi optimization approach for Pb(II) and Hg(II) removal from aqueous solutions using modified mesoporous carbon. *Journal of Hazardous Materials*, 2011, 192: 1046–1055. https://doi.org/10.1016/j.jhazmat.2011.06.006

[4] ANAGNOSTOPOULOS V.A., MANARIOTIS I. D., KARAPANAGIOTI H. K., and CHRYSIKOPOULOS C. V. Removal of mercury from aqueous solutions by malt spent rootlets. *Chemical Engineering Journal*, 2012, 213: 135–141. https://doi.org/10.1016/j.cej.2012.09.074

[5] CHOJNACKI A., CHOJNACKA K., HOFFMANN J., and GÓRECKI, H. The application of natural zeolites for mercury removal: from laboratory tests to industrial scale. *Minerals Engineering*, 2004, 17: 933–937. https://doi.org/10.1016/j.mineng.2004.03.002

[6] HUTCHISON A., ATWOOD D., and SANTILLIANN-JIMINEZ Q. E. The removal of mercury from water by open chain ligands containing multiple sulfurs. *Journal of Hazardous Materials*, 2008, 156: 458–465.

[7] LIU M., HOU L., XI B., ZHAO Y. and XIA X. Synthesis, characterization, and mercury adsorption properties of hybrid mesoporous aluminosilicate sieve prepared with fly ash. *Applied Surface Science*, 2013, 273: 706–716. https://doi.org/10.1016/j.apsusc.2013.02.116

[8] DABROWSKI A., HUBICKI Z., PODKOSCIELNY P., and ROBENS E. Selective removal of the heavy metal ions from waters and industrial wastewaters by ion-exchange method. *Chemosphere*, 2004, 56(2): 91–106. https://doi.org/10.1016/j.chemosphere.2004.03.006

[9] TAWABINI B., AL-KHALDI S., ATIEH M., and KHALED M. Removal of mercury from water by multi-walled carbon nanotubes. *Water Science and Technology*, 2010, 61: 591–598. https://doi.org/10.2166/wst.2010.897

[10] VUKOVIC G. D., MARINKOVIC A. D., COLIC M., RISTIC M. Đ., ALEKSIC R., PERIC-GRUJIC A. A., and USKOKOVIC P. S. Removal of cadmium from aqueous solutions by oxidized and ethylenediamine-functionalized multi-walled carbon nanotubes. *Chemical Engineering*

Journal, 2010, 157(1): 238-248. https://doi.org/10.1016/j.cej.2009.11.026

[11] ZHAO P., GUO X., and ZHENG C. Removal of elemental mercury by iodine-modified rice husk as sorbents. *Journal of Environmental Sciences*, 2010, 22: 1629–1636. https://doi.org/10.1016/S1001-0742(09)60299-0

[12] ALIJANI H., BEYKI M. H., SHARIATINIA Z., BAYAT M., and SHEMIRANI F. A new approach for one step syntesis of magnetic carbon nanotubes/diatomite earth composite by chemical vapor deposition method: application for removal of lead ions. *Chemical Engineering Journal*, 2014, 253: 456–463. http://dx.doi.org/10.1016/j.cej.2014.05.021

[13] BAYTAK S., & TÜRKER A. R. Determination of chromium, cadmium and manganese in water and fish samples after preconcentration using penicillium digitatum immobilized on pumice stone. *CLEAN - Soil Air Water*, 2009, 37: 314–318. http://dx.doi.org/10.1002/clen.200900037

[14] GHODBANE I., & HAMDAOUI O. Removal of mercury(II) from aqueous media using eucalyptus bark: kinetic and equilibrium studies. *Journal of Hazardous Materials*, 2008, 160(2-3): 301–309. https://doi.org/10.1016/j.jhazmat.2008.02.116

[15] MIRETZKY P., & CIRELLI A. F. Hg(II) removal from water by chitosan and chitosan derivatives: a review. *Journal of Hazardous Materials*, 2009, 167: 10–23. https://doi.org/10.1016/j.jhazmat.2009.01.060

[16] ABOLFAZL A., MOHAMMAD S., and SOODABEH S. Magnetic nanoparticles: preparation, physical, properties, and application in biomedicine. *Nanoscale Research Letters*, 2012, 7: 144.

[17] GUANG S. C., PEILONG W., XIN L., YUE W., GUILONG W., and JUNOING L. A sensitive nonenzymatic hydrogen peroxide sensor based on Fe_3O_4-Fe_2O_3 nanocomposites. *Bulletin of Materials Science*, 2014, 38: 1-5. http://dx.doi.org/10.1007/s12034-014-0803-x

[18] RAHMAWATI R., TAUFIQ A., SUNARYONO, FUAD A., YULIARTO B., SUYATMAN S., and KURNIADI D. Synthesis of Magnetite (Fe3O4) Nanoparticles from Iron sands by Co-precipitation-Ultrasonic Irradiation Methods. *Journal of Materials and Environmental Sciences*, 2018, 9: 155-160.

[19] SUK F. C., SUH C. P., CHING H. T. Green Synthesis of Magnetic Nanoparticle (via Thermal Decomposition Method) with Controllable Size and Shape. *Journal of Materials and Environmental Science*, 2011, 2: 299-302. https://www.jmaterenvironsci.com/Document/vol2/vol2_N3/25-JMES-85-2011-Chin.pdf

[20] INDRAYANA I. P. T., TUNY M. T., PUTRA R. A., JUHARNI, SUHARYADI E., KAT T., and IWATA S. Synthesis, Characterization and Application of Fe3O4 Nanoparticles As A Signal Amplifier Element in Surface Plasmon Resonance Biosensing *Jornal Online of Physics*, 2020, 5: 65-74. https://doi.org/10.22437/jop.v5i2.8259

[21] CHENG J. P., MA R., SHI D., and ZHANG X. B. Rapid growth of magnetite nanoplates by ultrasonic irradiation at low temperature. *Ultrasonics Sonochemistry*, 2011, 18: 1038-1042.

[22] PRASETYOWATI R., ARISWAN, WARSONO, and DEWI N. Synthesis and Characterization of Magnetite Nanoparticles (Fe3O4) Based on Iron Sand from Glagah Kulon Progo Yogyakarta via Coprecipitation Method with Variations in The Dissollution Duration. Proceedings of the Science and Science Education International Seminar Proceedings on Promoting Science for Technologi & Education Advancement, Semarang, 2019, pp. 1-5.

[23] MASCOLO M. C., PEI Y., and RING T. A. Room temperature co-precipitation synthesis of magnetite nanopartcles in a large pH window with different bases. *Materials*, 2013, 6: 5549-5567.

[24] NURHASANA S., IPUTU I., EDI S., KATO T., and IWATA S. Effect of Synthesis Temperature and NaOH Concentration on Microstructural and Magnetic Properties of $Mn_{0.5}Zn_{0.5}Fe_2O_4$ Nanoparticles. *IoP on Materials Science and Engineering*, 2017, 202: 012048.

[25] DESKA L. P., GITA S., HARLINA A., and MOHAMAD S. A. Characteristics and Mineral Content of Lampung Tengah Iron sand. *Journal of Science and Applicative Technology*, 2018, 2(1): 192-196. https://doi.org/10.35472/281488

[26] RIANNA M., SEMBIRING T., SITUMORANG M., KURNIAWAN C., SETIADI E. A., TETUKO A. P., SIMBOLON S., MASNO G., and PERDAMEAN S. Preparation and Characterization of Natural Iron Sand from Kata Beach, Sumatera Barat Indonesia with High Energy Milling (HEM). *Jurnal Natural*, 2018, 18: 97-100. http://dx.doi.org/10.24815/jn.v18i2.11163

[27] DARVINA Y., RIFAI D., and RAMLI. Synthesis of Magnetite Nanoparticle from Iron Sand by ball-milling. *Journal of Physics: Conference Series*, 2019, 1185: 1-5.

[28] SADJAB, B. A., INDRAYANA, I. P. T., LIWAMONY, S., and UMAM, R. Investigation of The Distribution and Fe Content of Iron Sand at Wari Ino Beach Tobelo Using Resistivity Method with Werner-Schlumberger Configuration. *Jurnal Ilmiah Pendidikan Fisika Al-Biruni*, 2020, 9(1): 141–160. https://doi.org/10.24042/jipfalbiruni.v9i1.5394

[29] KURNIA K., KASESIDE M., and IWAMONY S. Study Microstructure of Fe_3O_4 Modification Using PEG 4000 form Iron Sand at Wari Ino Beach As A Biosensor Application. *Indonesian Journal of Chemical Research*, 2021, 8(3): 168–171. https://doi.org/10.30598//ijcr.2021.8-kur

[30] ZHANG L., WU H. B., and LOU X. W. Iron-Oxide-Based Advanced Anode Materials for Lithium-Ion. *Advanced Energy Materials*, 2014, 4: 1300958. https://doi.org/10.1002/aenm.201300958

[31] EDI S, HERMAWAN, and PUSPITARUM. Crystal Structure and Magnetic Properties of Magnesium Ferrite Nanoparticles Synthesized by Coprecipitation Method *Journal of Physics: Conference Series*, 2018, 1091: 012003.

[32] WIDANARTO W., SAAHAR M. R., GHOSHAL S. K., ARIFIN R., ROHANI M. S., and HAMZAH K. Effect of Natural Fe_3O_4 nanoparticles on structural and optical properties of Er^{3+} doped tellurite glass. *Journal of Magnetism and Magnetic Materials*, 2013, 326: 123-128.

[33] INDRAYANA I. P. T., TJUANA L. A., TUNY M. T., and KURNIA. Nanostructure and Optical Properties of Fe3O4: Effect of Calcination Temperature and Dwelling Time. *Journal of Physics: Conference Series*, 2019, 1341: 1-9.

[34] EL GHANDOOR H., ZIDAN H. M., KHALIL M. M. H., and ISMAIL M. I. M. Synthesis and some physical properties of magnetite (Fe_3O_4) Nanoparticles. *International Journal of Electhrochemical Sience*, 2012, 7: 5734-5745. http://www.electrochemsci.org/papers/vol7/7065734.pdf

[35] WIATROWSKI, H. A., DAS, S., KUKKADAPU, R., ILTON, E. S., BARKAY, T., and YEE, N. Reduction of Hg(II) to Hg(0) by magnetite. *Environmental Science & Technology*, 2009, 43: 5307–5313. https://doi.org/10.1021/es9003608
[36] PASAKARNIS, T. S., BOYANOV, M. I., KEMNER, K. M., MISHRA, B., O'LOUGHLIN, E. J., PARKIN, G., and SCHERER, M. M. Influence of chloride and Fe(II) content on the reduction of Hg(II) by magnetite. *Environmental Science & Technology*, 2013, 47: 6987–6994. https://doi.org/10.1021/es304761u
[37] GANGULY, M., DIB, S., and ARIYA A. Fast, Cost-effective and Energy Efficient Mercury Removal-Recycling Technology. *Scientific Reports*, 2018, 8: 16255. https://doi.org/10.1038/s41598-018-34172-6
[38] MATHZW D. S., & JUANG R. S. An overview of the Structure and Magnetism of Spinel Ferrite Nanoparticle and Their Synthesis in Microemulsions. *Chemical Engineering Journal*, 2007, 129: 51-65. https://doi.org/10.1016/j.cej.2006.11.001
[39] HASANY S. F., ABDURRAHMAN N. H., SUNARTI A. R., and JOSE R. Magnetic Iron Oxide Nanoparticles: Chemical Synthesis and Applications Review. *Current Nanoscience*, 2013, 9: 561-575. http://dx.doi.org/10.2174/15734137113099990085
[40] AHMED M. A., ALI S. M., EL-DEK S. I., and GALAL A. Magnetite-hematite nanoparticles prepared by green methods for heavy metal ions removal from water. *Materials Science and Engineering: B*, 2013, 178(10): 744-751. https://doi.org/10.1016/j.mseb.2013.03.011
[41] WANG X., SUN R., and WANG C. Ph dependence and thermodynamics of Hg (II) adsorption onto chitosan-poly(vinyl alcohol) hydrogen adsoerbent. *Colloids and Surfaces A Physicochemical and Engineering Aspects*, 2014, 441: 51-58. http://dx.doi.org/10.1016/j.colsurfa.2013.08.068
[42] GHAZEMI Z., SEIF A., AHMADI T. S., ZARGAR B., RASHIDI F. and ROUZBAHANI G. M. Thermodynamic and kinetic studies for the adsorption of Hg(II) by nano-TiO2 from aqueous solution. *Advanced Powder Technology*, 2012, 23(2): 148-156. https://doi.org/10.1016/j.apt.2011.01.004
[43] RAJI F., & PAKIZEH M. Kinetic and thermodynamic studies of Hg(II)adsorption onto MCM-41 modified by ZnCl2. *Applied Surface Science*, 2014, 301: 568-575. https://doi.org/10.1016/j.apsusc.2014.02.136
[44] CUI L., WANG Y., GAO L., HU L., YAN L., WEI Q., and DU B. EDTA functionalized magnetic graphene oxide for removal of Pb(II), Hg(II) and Cu(II) in water treatment: Adsorption mechanism and separation property. *Chemical Engineering Journal*, 2015, 281: 1–10. https://doi.org/10.1016/j.cej.2015.06.043
[45] SHAN C., MA Z., TONG M., and NI J. Removal of Hg(II) by poly(1-vinylimidazole)-grafted Fe3O4@SiO2 magnetic nanoparticles. *Water Research*, 2015, 69: 252–260. https://doi.org/10.1016/j.watres.2014.11.030
[46] LÓPEZ-MUÑOZ M.-J., ARENCIBIA A., CERRO L., PASCUAL R., and MELGAR Á. Adsorption of Hg(II) from aqueous solutions using TiO2 and titanate nanotube adsorbents. *Applied Surface Science*, 2016, 367: 91–100. https://doi.org/10.1016/j.apsusc.2016.01.109
[47] WANG Z., XU J., HU Y., ZHAOU J., LIU Y., LOU Z., and XU X. Functional nanomaterials: Study on aqueous Hg(II) adsorption by magnetic Fe3O4@SiO2-SH nanoparticles. *Journal of the Taiwan Institute of Chemical Engineers*, 2016, 60: 394-402.

参考文:

[1] AZIZI S. N., ROOZBEHANI DEHNAVI A., 和 JOORABDOOZHA A. 使用裸壳二氧化硅的内衬一种型纳米沸石的合成和表征：从标准溶液和实际溶液中去除汞。材料研究通报，2013, 48: 1753-1759. https://doi.org/10.1016/j.materresbull.2012.12.068
[2] JIMENEZ-JIMENEZ J, ALGARRA M., RODRIGUEZ-CASTELLON E., JIMENEZ-LOPEZ A. 和 ESTEVES DA SILVA J. C. G. 杂化多孔酸盐异质结构作为工业污水中(汞(II)和镍（二）的吸附剂。有害材料杂志, 2011, 190(1-3): 694-699. https://doi.org/10.1016/j.jhazmat.2011.03.110
[3] ZOLFAGHARI G., ESMAILI-SARI A., ANBIA M., YOUNESI H., AMIRMAHMOODI S., 和 GHAFARI-NAZARI A. 使用改良的介孔碳从水溶液中去除铅(II)和汞(II)的田口优化方法。危险材料杂志, 2011, 192: 1046–1055. https://doi.org/10.1016/j.jhazmat.2011.06.006
[4] ANAGNOSTOPOULOS V.A., MANARIOTIS I. D., KARAPANAGIOTI H. K., 和 CHRYSIKOPOULOS C. V. 通过麦芽废细根去除水溶液中的汞。化学工程杂志, 2012, 213: 135–141. https://doi.org/10.1016/j.cej.2012.09.074
[5] CHOJNACKI A., CHOJNACKA K., HOFFMANN J., 和 GÓRECKI, H. 天然沸石去除汞的应用：从实验室测试到工业规模。矿产工程，2004, 17: 933–937. https://doi.org/10.1016/j.mineng.2004.03.002
[6] HUTCHISON A., ATWOOD D., 和 SANTILLIANN-JIMINEZ Q. E. 通过含有多种硫的开链配体从水中去除汞。危险材料杂志, 2008, 156: 458–465.
[7] LIU M., HOU L., XI B., ZHAO Y. 和 XIA X. 粉煤灰制备杂化介孔硅铝酸盐筛的合成、表征及汞吸附性能. 应用表面科学，2013, 273: 706–716. https://doi.org/10.1016/j.apsusc.2013.02.116
[8] DABROWSKI A., HUBICKI Z., PODKOSCIELNY P., 和 ROBENS E. 从离子交换法中选择性去除水和工业废水中的重金属离子。化学圈，2004, 56(2): 91–106. https://doi.org/10.1016/j.chemosphere.2004.03.006
[9] TAWABINI B., AL-KHALDI S., ATIEH M., 和 KHALED M. 多壁碳纳米管从水中清除汞。水科学技术, 2010, 61: 591–598. https://doi.org/10.2166/wst.2010.897
[10] VUKOVIC G. D., MARINKOVIC A. D., COLIC M., RISTIC M. Đ., ALEKSIC R., PERIC-GRUJIC A. A., 和 USKOKOVIC P. S. 通过氧化和乙二胺功能化的多壁碳纳米管从水溶液中去除。化学工程杂志, 2010, 157(1): 238-248. https://doi.org/10.1016/j.cej.2009.11.026
[11] ZHAO P., GUO X., 和 ZHENG C. 修改作稻壳,作为吸附剂去除元素汞。环境科学杂志, 2010, 22: 1629–1636. https://doi.org/10.1016/S1001-0742(09)60299-0
[12] ALIJANI H., BEYKI M. H., SHARIATINIA Z., BAYAT M., 和 SHEMIRANI F. 化学气相沉积法一步合成磁性碳纳米管/硅藻土组合物的新方法：应用于去除铅离子。化学工程杂志，2014, 253: 456–463. http://dx.doi.org/10.1016/j.cej.2014.05.021
[13] BAYTAK S., & TÜRKER A. R. 使用固定在浮石石上的青霉素数字化的风格,水和鱼样品中的长泽和储藏物进

行试测，干净-土壤水，2009, 37: 314–318. http://dx.doi.org/10.1002/clen.200900037
[14] GHODBANE I., & HAMDAOUI O. 使用桉树树皮从水性介质中去除汞(II)：动力学和平衡研究。危险材料杂志，2008, 160(2-3): 301–309. https://doi.org/10.1016/j.jhazmat.2008.02.116
[15] MIRETZKY P., & CIRELLI A. F. 汞(II)通过壳聚糖和壳聚糖衍生物从水中清除：综述。危险材料杂志, 2009, 167: 10–23. https://doi.org/10.1016/j.jhazmat.2009.01.060
[16] ABOLFAZL A., MOHAMMAD S., 和 SOODABEH S. 磁性纳米粒子：制备、物理、性质和在生物医学中的应用。纳米研究快报, 2012, 7: 144.
[17] GUANG S. C., PEILONG W., XIN L., YUE W., GUILONG W., 和 JUNOING L. 基于四氧化三铁-三氧化二铁纳米复合材料的敏感非咬过氧化氢传感器。材料科学公告，2014, 38: 1-5. http://dx.doi.org/10.1007/s12034-014-0803-x
[18] RAHMAWATI R., TAUFIQ A., SUNARYONO, FUAD A., YULIARTO B., SUYATMAN S., 和 KURNIADI D. 通过共沉淀超声 φ 照法从铁砂中合成磁铁矿(四氧化三铁)纳米颗粒。材料与环境科学杂志, 2018, 9: 155-160.
[19] SUK F. C., SUH C. P., CHING H. T. 尺寸和形状可控的磁性纳米粒子的绿色合成（通过热分解法）。材料与环境科学杂志，2011, 2: 299-302. https://www.jmaterenvironsci.com/Document/vol2/vol2_N3/25-JMES-85-2011-Chin.pdf
[20] INDRAYANA I. P. T., TUNY M. T., PUTRA R. A., JUHARNI, SUHARYADI E., KAT T., 和 IWATA S. 四氧化三铁纳米粒子的合成、表征及在表面等离子共振生物传感中作为信号放大元件的应用，2020, 5: 65-74. https://doi.org/10.22437/jop.v5i2.8259
[21] CHENG J. P., MA R., SHI D., 和 ZHANG X. B. 低温超声筱照快速生长磁铁矿纳米片。超声波声化学, 2011, 18: 1038-1042.
[22] PRASETYOWATI R., ARISWAN, WARSONO, 和 DEWI N. 基于来自格拉加库隆普罗戈日惹的铁砂的磁铁矿纳米颗粒(四氧化三铁)的合成和表征，通过共沉淀法改变溶解持续时间。科学与科学教育国际研讨会论文集, 促进科学技术与教育进步, 三宝垄, 2019 年，第 1-5 页.
[23] MASCOLO M. C., PEI Y., 和 RING T. A. 在不同碱的大酸碱度窗口中室温共沉淀合成磁铁矿纳米颗粒。材料, 2013, 6: 5549-5567.
[24] NURHASANA S., IPUTU I., EDI S., KATO T., 和 IWATA S. 合成温度和氢氧化钠浓度对 $Mn_{0.5}Zn_{0.5}Fe_2O_4$ 纳米粒子的微观结构和磁性的影响。材料科学与工程物理研究所, 2017, 202: 012048.
[25] DESKA L. P., GITA S., HARLINA A., 和 MOHAMAD S. A. 中央灯笼铁砂的特性和矿物质含量。科学与应用技术杂志，2018, 2(1): 192-196. https://doi.org/10.35472/281488
[26] RIANNA M., SEMBIRING T., SITUMORANG M., KURNIAWAN C., SETIADI E. A., TETUKO A. P., SIMBOLON S., MASNO G., 和 PERDAMEAN S. 印度尼西亚西苏门答腊岛卡塔海滩天然铁砂的高能研磨制备与表征。自然杂志，2018, 18: 97-100. http://dx.doi.org/10.24815/jn.v18i2.11163
[27] DARVINA Y., RIFAI D., 和 RAMLI. 通过球磨法从铁砂中合成磁铁矿纳米颗粒。物理学杂志：会议系列, 2019, 1185: 1-5.
[28] SADJAB, B. A., INDRAYANA, I. P. T., LIWAMONY, S., 和 UMAM, R. 使用电阻率法和沃纳-斯伦贝谢配置调查瓦里伊诺海滩托韦洛铁砂的分布和铁含量。比鲁尼物理教育科学杂志，2020, 9(1): 141–160. https://doi.org/10.24042/jipfalbiruni.v9i1.5394
[29] KURNIA K., KASESIDE M., 和 IWAMONY S. 研究四氧化三铁修饰的微观结构，使用在瓦里伊诺海滩上以生物传感器的应用，使用聚乙烯 4000 形成铁砂。印尼化学研究杂志，2021, 8(3): 168–171. https://doi.org/10.30598//ijcr.2021.8-kur
[30] ZHANG L., WU H. B., 和 LOU X. W. 松离子的铁氧化物为晚期阳极材料。高级能源材料, 2014, 4: 1300958. https://doi.org/10.1002/aenm.201300958
[31] EDI S, HERMAWAN, 和 PUSPITARUM. 共沉淀法合成铁氧体纳米粒子的晶体结构和磁性物理学杂志：会议系列, 2018, 1091: 012003.
[32] WIDANARTO W., SAAHAR M. R., GHOSHAL S. K., ARIFIN R., ROHANI M. S., 和 HAMZAH K. 天然四氧化三铁纳米粒子对 Er3+掺杂亚碲酸盐玻璃结构和光学性能的影响。磁性与磁性材料学报, 2013, 326: 123-128.
[33] INDRAYANA I. P. T., TJUANA L. A., TUNY M. T., 和 KURNIA. 四氧化三铁的纳米结构和光学特性：钙化温度和住宅时间的影响。物理杂志：会议系列，2019, 1341: 1-9.
[34] EL GHANDOOR H., ZIDAN H. M., KHALIL M. M. H., 和 ISMAIL M. I. M. 磁铁矿（四氧化三铁）纳米颗粒的合成和某些物理特性。国际电化学杂志, 2012, 7: 5734-5745. http://www.electrochemsci.org/papers/vol7/7065734.pdf
[35] WIATROWSKI, H. A., DAS, S., KUKKADAPU, R., ILTON, E. S., BARKAY, T., 和 YEE, N. 磁铁矿将汞(II)还原为汞(0)。环境科学与技术，2009, 43: 5307–5313. https://doi.org/10.1021/es9003608
[36] PASAKARNIS, T. S., BOYANOV, M. I., KEMNER, K. M., MISHRA, B., O'LOUGHLIN, E. J., PARKIN, G., 和 SCHERER, M. M. 氯化物和铁(II)含量对磁铁矿还原汞(II)的影响。环境科学与技术，2013, 47: 6987–6994. https://doi.org/10.1021/es304761u
[37] GANGULY, M., DIB, S., 和 ARIYA A. 快速、经济且节能的汞去除回收技术。科学报告，2018, 8: 16255. https://doi.org/10.1038/s41598-018-34172-6
[38] MATHZW D. S., & JUANG R. S. 尖晶石铁氧体纳米粒子的结构和磁性及其在微乳液中的合成概述。化学工程杂志，2007, 129: 51-65. https://doi.org/10.1016/j.cej.2006.11.001
[39] HASANY S. F., ABDURRAHMAN N. H., SUNARTI A. R., 和 JOSE R. 磁性氧化铁纳米粒子：化学合成和应用综述。当前的纳米科学，2013, 9: 561-575. http://dx.doi.org/10.2174/15734137113099990085
[40] AHMED M. A., ALI S. M., EL-DEK S. I., 和 GALAL A. 由绿色方法制备的磁铁矿-透明石纳米颗粒从水中清除重金属离子。材料科学与工程：乙, 2013, 178(10): 744-751. https://doi.org/10.1016/j.mseb.2013.03.011

[41] WANG X., SUN R., 和 WANG C. 汞（二） 吸附到壳聚糖-聚（乙烯醇）氢吸附剂上的博士依赖性和热力学。胶体和表面物理化学和工程方面，2014，441：51-58. http://dx.doi.org/10.1016/j.colsurfa.2013.08.068
[42] GHAZEMI Z., SEIF A., AHMADI T. S., ZARGAR B., RASHIDI F. 和 ROUZBAHANI G. M. 纳米二氧化钛研究水溶液中吸附汞(II)的热力学和动力学研究。先进的粉末技术，2012，23(2)：148-156. https://doi.org/10.1016/j.apt.2011.01.004
[43] RAJI F., & PAKIZEH M. 氯化锌 改性的物质 41 美组合物吸附汞(II)的动力学和热力学研究。应用表面科学，2014，301：568-575. https://doi.org/10.1016/j.apsusc.2014.02.136
[44] CUI L., WANG Y., GAO L., HU L., YAN L., WEI Q., 和 DU B. 乙二胺四乙酸乙二氮四乙酸功能化磁性氧化石墨烯用于去除水处理中的铅(II)、汞(II)和铜(II)：吸附机理和分离性能。化学工程杂志，2015，281：1–10. https://doi.org/10.1016/j.cej.2015.06.043
[45] SHAN C., MA Z., TONG M., 和 NI J. 聚（1-乙烯基喵)接枝的 Fe3O4@SiO2 磁性纳米粒子去除汞(II)。水研究，2015，69：252–260. https://doi.org/10.1016/j.watres.2014.11.030
[46] LÓPEZ-MUÑOZ M.-J., ARENCIBIA A., CERRO L., PASCUAL R., 和 MELGAR Á. 纳米二氧化钛从水溶液中吸附汞(II)的热力学和动力学。先进的粉末技术，2016，367：91–100. https://doi.org/10.1016/j.apsusc.2016.01.109
[47] WANG Z., XU J., HU Y., ZHAOU J., LIU Y., LOU Z., 和 XU X. 功能性纳米材料：磁性 FE_3O_4@SiO_2-SH 纳米颗粒对水溶液(II)吸附的研究。台湾化学工程师学院杂志，2016，60：394-402.